

# Cross-Layer Design of Random On-Off Accumulative Transmission with Iterative Detections

Jingxian Wu\*, *Member, IEEE* and Geoffrey Ye Li†, *Fellow, IEEE*

\* Department of Electrical Engineering, University of Arkansas, Fayetteville, AR 72701, USA.

† School of Electrical and Computer Engineering, Georgia Institute of Technology, Atlanta, GA 30332, USA.

**Abstract**—Random on-off accumulative transmission (R-OOAT) is a cross-layer technique that can achieve collision-tolerance in the media access control (MAC) layer by leveraging on the signal processing capability in the physical (PHY) layer. In this paper, a new PHY/MAC cross-layer design is proposed for the R-OOAT framework. In the PHY layer, we propose an iterative method for the detection of R-OOAT signals colliding at the receiver, such that the transmitted information can be recovered with a low complexity in the presence of severe signal collisions. The iterative detection is enabled by the unique signal structure of the R-OOAT, and it can operate in both coded and uncoded systems. In the MAC layer, the R-OOAT scheme uses silence periods inside a frame to achieve collision-tolerance, which is different from most conventional MAC schemes that rely on random intervals between frames to reduce collision. The theoretical spectral efficiency of R-OOAT is analyzed with the PHY/MAC operations. Analytical and simulation results show that the proposed cross-layer design can support more users and achieve a much higher spectral efficiency compared to conventional MAC schemes.

## I. INTRODUCTION

Cross-layer design of wireless communication networks has attracted a great attention during the last decade for its potential to provide significant increase in end-to-end throughput, scalable network performance, and satisfactory quality of services. A large family of cross-layer techniques for wireless networks are developed by performing joint design across the physical (PHY) and media access control (MAC) layers.

Existing PHY/MAC cross-layer design methods can be roughly divided into two categories. The first category is PHY-aware MAC, where the MAC layer protocols adjust their operations based on the knowledge of PHY layer parameters, such as adaptive rate control, adaptive power control, and opportunistic scheduling [1] - [3], etc. The second category utilizes signal processing capability in the PHY layer to improve the performance in the MAC layer. Many works in the second category are heralded by the concept of multipacket reception (MPR) [4] - [6], where the PHY layer can correctly decode a fraction of multiple transmissions, with multiuser detection and/or interference cancellation. Most of the MPR related studies are performed with a traditional PHY layer structure, such as code division multiple access (CDMA) [7], time hopping ultra-wide band (TH-UWB) [8], and minimum mean-square-error (MMSE) or zero-forcing (ZF) detectors [9]

- [10]. In order to exploit the full potential of the PHY/MAC interactions, it is desirable to design completely new PHY and MAC operations tailored for cross-layer design.

In this paper, we propose a new PHY/MAC cross-layer design based on the framework of the collision-tolerant MAC (CT-MAC) [11], [12], where the collision tolerance in the MAC layer is achieved by employing an on-off accumulative transmission (OOAT) scheme in the PHY layer. In OOAT, each data symbol is transmitted in the form of multiple identical sub-symbols (accumulative transmission), and two sub-symbols are separated by a silence period (on-off transmission). In [11], [12], the detection of the OOAT signals is performed by using an enhanced Viterbi algorithm with a time-varying trellis, the complexity of which becomes prohibitively high when the number of users is large. To address this problem, we propose a low complexity iterative detection method in the PHY layer by utilizing the unique signal structure of the random OOAT (R-OOAT) scheme. The new iterative detection method can operate in both coded and uncoded systems, whereas most existing iterative detection methods can only operate in coded systems in the form of turbo equalization.

In the MAC layer, the data are divided into frames and transmitted in succession without intervals unless there is no data to transmit. This is different from most conventional MAC schemes that use random intervals between frames to reduce collision. The R-OOAT uses structured silence periods inside a frame to achieve collision tolerance. The MAC layer performance of the R-OOAT scheme is studied theoretically in term of spectral efficiency. It is shown by both theoretical analysis and simulation that the new PHY/MAC design of CT-MAC can support more users and achieve a much higher spectral efficiency compared to the well-known slotted ALOHA scheme.

## II. RANDOM ON-OFF ACCUMULATIVE TRANSMISSION

In this section, we briefly review the model and operations of R-OOAT [12]. Consider a wireless sensor network (WSN) with  $N$  spatially distributed nodes and one base station (BS). Data collected by the sensor nodes are delivered to the BS through a one-hop transmission. To achieve collision tolerance in the MAC layer, the wireless nodes employ the R-OOAT scheme in the PHY layer as shown in Fig. 1. Each data symbol in the R-OOAT scheme is transmitted through  $R$  identical sub-symbols with a duration of  $T_0$  each. The symbol period is  $T_s =$

$MT_0$  with  $M \geq R$ . Consequently,  $R$  out of  $M$  sub-symbol positions are occupied during one symbol period. The positions of the occupied sub-symbols or the transmission pattern for the  $n$ -th user can be expressed by a binary vector of length  $M$ ,  $\mathbf{p}_n = [p_n(1), \dots, p_n(M)]^T \in \mathcal{B}^{M \times 1}$ , where  $\mathcal{B} = \{0, 1\}$ , with  $p_n(m) = 1$  if a sub-symbol is transmitted at the  $m$ -th sub-symbol location, and  $p_n(m) = 0$  otherwise.

The R-OOAT scheme is defined by ternary  $N, M$ , and  $R$ . Fig. 1 shows an example of a system with  $N = 5$ ,  $M = 12$ , and  $R = 4$ . Due to the asynchronism among the nodes and the on-off property of the scheme, only a subset of the nodes will mutually interfere with each other at a given sub-symbol position.

Define the collision order at the sub-symbol position  $m$  as  $N_c(m) = \sum_{n=1}^N p_n(i_{nm})$ , where  $i_{nm} = \text{mod}_M(m) - p_{n0}$ , with  $\text{mod}_M(m)$  being the modular  $M$  operator, and  $p_{n0}$  is the relative starting position of the  $n$ -th node due to the node asynchronism. For example, in Fig. 1,  $p_{10} = 2$  and  $p_{20} = 1$ . The collision order is defined as  $N_c = \max_m N_c(m)$ . We have  $N_c = 2$  for the system shown in Fig. 1.

Based on the above discussion, a CT-MAC system with R-OOAT can be represented by

$$y(m) = \sum_{n=1}^N p_n(i_{nm}) h_n s_{nk_{nm}} + z(m) \quad (1)$$

where  $y(m)$  and  $z(m)$  are the received sample and additive white Gaussian noise (AWGN) at the  $m$ -th sub-symbol, respectively,  $h_n$  is the fading coefficient between node  $n$  and the BS,  $s_{nk}$  is the  $k$ -th symbol transmitted by node  $n$ , and  $k_{nm} = \lceil \frac{m-p_{n0}}{M} \rceil$ , with  $\lceil a \rceil$  being the smallest integer greater than or equal to  $a$ .

A WSN is called collision-tolerant if the transmitted signals can be recovered at the receiver beyond a certain fidelity measure. For a CT-MAC system with the R-OOAT, each received sample is the weighted superposition of symbols from up to  $N_c$  different nodes at any moment. At the mean time, each symbol,  $s_{nk}$ , is embedded in  $R$  received samples at the receiver. This is equivalent to a  $N_c$ -input  $R$ -output system. In practice, to ensure collision tolerance and system performance, it is desirable to have a symmetric or over-determined system with  $N_c \leq R$ .

With asynchronous nodes, the symbol from one node usually collides with multiple symbols from multiple nodes, and the colliding symbols change from sample to sample. The optimum detection in this case should be maximum likelihood sequence estimation (MLSE). Due to the random structure of the position vectors and the asynchronous nature of the system, the interference changes with respect to time. Therefore, the system will have a time-varying trellis structure. At the BS, the detection in the PHY layer can be performed by applying the extended Viterbi algorithm with a time-varying trellis as described in [11]. However, the complexity of the optimum algorithm scales with  $S^N$ , where  $S$  is the modulation constellation size, and  $N$  is the number of users. The complexity could be prohibitively high when  $S$  or  $N$  is large.

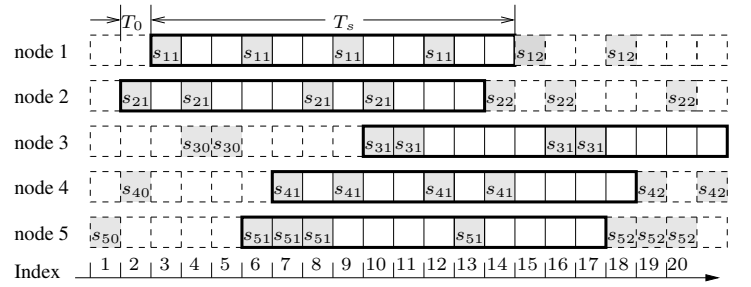


Fig. 1. An R-OOAT system with  $N = 5$  nodes,  $R = 4$  repetitions per symbol period, and each symbol contains  $M = 12$  possible sub-symbol positions.

### III. ITERATIVE DETECTION WITH SUCCESSIVE SOFT INTERFERENCE CANCELLATION

In this section, we propose a new iterative detection method with successive soft interference cancellation (SSIC), which will be used by the BS to extract the information from the signals colliding at the receiver.

The iterative detection method is developed by utilizing the signal structure of the R-OOAT. For a R-OOAT system with parameters  $N, M$ , and  $R$ , divide the received samples into blocks, such that each block contains  $M$  samples. The received sample vector in the  $k$ -th block can then be written as

$$\mathbf{y}_k = \mathbf{C}_0 \cdot \mathbf{F} \cdot \mathbf{s}_{k-1} + \mathbf{C}_1 \cdot \mathbf{F} \cdot \mathbf{s}_k + \mathbf{z}_k \quad (2)$$

where  $\mathbf{y}_k = [y_{kM+1}, \dots, y_{kM+M}]^T \in \mathcal{C}^{M \times 1}$ ,  $\mathbf{z}_k = [z_{kM+1}, \dots, z_{kM+M}]^T \in \mathcal{C}^{M \times 1}$  are the signal sample vector and AWGN vector, respectively,  $\mathbf{s}_k = [s_{1k}, s_{2k}, \dots, s_{Nk}]^T \in \mathcal{C}^{N \times 1}$  is the multi-user signal vector of the  $k$ -th symbol, and  $\mathbf{F} = \text{diag}\{\mathbf{h}\} \in \mathcal{C}^{N \times N}$  is a diagonal matrix with  $\mathbf{h} = [h_1, \dots, h_N]^T$  on its main diagonal. The effects of the position vectors are represented in the position matrices,  $\mathbf{C}_i \in \mathcal{B}^{M \times N}$ , for  $i = 0, 1$ . The  $(m, n)$ -th element of  $\mathbf{C}_0$  is 1 if  $s_{n(k-1)}$  from the  $n$ -th user is transmitted at the sub-symbol location  $kM+m$ , and 0 otherwise.  $\mathbf{C}_1$  is defined similarly based on  $s_{nk}$ .

For example, consider the system described in Fig. 1. If we group the samples from the first  $M = 12$  sub-symbol positions into a block, then the position matrices  $\mathbf{C}_0$  and  $\mathbf{C}_1$  can be written as

$$\mathbf{C}_0 = \begin{pmatrix} 0 & 0 & 0 & 0 & 1 \\ 0 & 0 & 0 & 1 & 0 \\ 0 & 0 & 0 & 0 & 0 \\ 0 & 0 & 1 & 0 & 0 \\ 0 & 0 & 1 & 0 & 0 \\ 0 & 0 & 0 & 0 & 0 \\ 0 & 0 & 0 & 0 & 0 \\ 0 & 0 & 0 & 0 & 0 \\ 0 & 0 & 0 & 0 & 0 \\ 0 & 0 & 0 & 0 & 0 \\ 0 & 0 & 0 & 0 & 0 \\ 0 & 0 & 0 & 0 & 0 \end{pmatrix}, \quad \mathbf{C}_1 = \begin{pmatrix} 0 & 0 & 0 & 0 & 0 \\ 0 & 1 & 0 & 0 & 0 \\ 1 & 0 & 0 & 0 & 0 \\ 0 & 1 & 0 & 0 & 0 \\ 0 & 0 & 0 & 0 & 0 \\ 1 & 0 & 0 & 0 & 1 \\ 0 & 0 & 0 & 1 & 1 \\ 0 & 1 & 0 & 0 & 1 \\ 1 & 0 & 0 & 1 & 0 \\ 0 & 1 & 1 & 0 & 0 \\ 0 & 0 & 1 & 0 & 0 \\ 1 & 0 & 0 & 1 & 0 \end{pmatrix}. \quad (3)$$

In the  $k$ -th block, the matrices  $\mathbf{C}_0$  and  $\mathbf{C}_1$  correspond to the transmission positions of the previous symbol vector,  $\mathbf{s}_{k-1}$ , and the current symbol vector,  $\mathbf{s}_k$ , respectively. The sum of the number of 1s on the  $n$ -th columns of  $\mathbf{C}_0$  and  $\mathbf{C}_1$  is always  $R$ . It should be noted that in order to write the system equation

in the form of (2), the block should be chosen in such a way that the samples in each block are contributed by at most two symbol vectors,  $\mathbf{s}_{k-1}$  and  $\mathbf{s}_k$ . This requirement can always be met since there are at most 2 different symbols for each user transmitted during  $M$  sub-symbol positions.

With the system model given in (2), there are both inter-block interference (IBI) between  $\mathbf{s}_{k-1}$  and  $\mathbf{s}_k$ , and co-channel interference (CCI) among the symbols inside  $\mathbf{s}_k$ . We propose to detect each block separately, where one symbol vector,  $\mathbf{s}_k$ , is detected by using one sample block,  $\mathbf{y}_k$ . With this block-wise detection, the IBI can be removed by subtracting the soft decisions from the previous block. The CCI among the symbols inside  $\mathbf{s}_k$  can be mitigated by employing a soft-input soft-output (SISO) equalizer. The SISO equalizer can be implemented with any equalizer that supports soft information processing. In this paper, the SISO-BDFE [13] is used as the SISO equalizer.

For the  $k$ -th block, the soft-input to the SISO equalizer is the *a priori* probability of the symbols,  $P(s_{nk} = S_i)$ , for  $n = 1, \dots, N$  and  $i = 1, \dots, S$ , where  $S_i \in \mathcal{S}$  with  $\mathcal{S}$  being the modulation constellation set with cardinality  $S$ . The *a priori* information is obtained from the previous detection round with an iterative detection method, and details will be given later in this section. The soft-output of the equalizer is the *a posteriori* probability of the symbols,  $P(s_{nk} = S_i | \mathbf{y}_k)$ , for  $n = 1, \dots, N$  and  $i = 1, \dots, S$ . With the soft-output at the equalizer output, define the *a posteriori* mean,  $\hat{s}_{nk}$ , and the extrinsic information,  $\beta_{nk}$ , of the symbol  $s_{nk}$  as

$$\hat{s}_{nk} = \sum_{i=1}^S P(s_{nk} = S_i | \mathbf{y}_k) S_i \quad (4a)$$

$$\beta_{nk}(i) = \log_2 P(s_{nk} = S_i | \mathbf{y}_k) - \log_2 P(s_{nk} = S_i) \quad (4b)$$

The extrinsic information will be used as the *a priori* input for the SISO equalization of  $s_{nk}$  in the next round of the iterative detection.

The *a posteriori* mean vector,  $\hat{\mathbf{s}}_k = [\hat{s}_{1k}, \dots, \hat{s}_{Nk}]^T \in \mathbb{C}^{N \times 1}$ , is the soft decision, and it is employed during the IBI cancellation as

$$\hat{\mathbf{y}}_k = \mathbf{y}_k - \mathbf{C}_0 \cdot \mathbf{F} \cdot \hat{\mathbf{s}}_{k-1}. \quad (5)$$

If the past detection is assumed to be correct, the signal after IBI cancellation can be written as

$$\hat{\mathbf{y}}_k = \mathbf{C}_1 \cdot \mathbf{F} \cdot \mathbf{s}_k + \mathbf{z}_k \quad (6)$$

Then the SISO equalizer can be applied to  $\hat{\mathbf{y}}_k$  in (6) by treating  $\mathbf{H}_1 = \mathbf{C}_1 \cdot \mathbf{F}$  as the channel matrix, and the result is the *a posteriori* mean and extrinsic information of  $\mathbf{s}_k$  as in (4).

The above procedures will be repeated until the end of a detection window containing  $K$  blocks. Since  $\mathbf{s}_{k-1}$  is detected before  $\mathbf{s}_k$ , we denote the IBI cancellation in (5) as forward SSIC. In the above procedures, the matrix  $\mathbf{C}_0$  is used for IBI cancellation, and the matrix  $\mathbf{C}_1$  is used for CCI cancellation.

Once we reach the end of a detection window, we can reverse the detection order by detecting  $\mathbf{s}_K$  first and  $\mathbf{s}_1$  last. In this case,

the IBI cancellation will be performed with a backward SSIC as

$$\hat{\mathbf{y}}_k^{(B)} = \mathbf{y}_k - \mathbf{C}_1 \cdot \mathbf{F} \cdot \hat{\mathbf{s}}_k \approx \mathbf{C}_0 \cdot \mathbf{F} \cdot \hat{\mathbf{s}}_{k-1} + \mathbf{z}_k. \quad (7)$$

After the IBI cancellation,  $\mathbf{s}_{k-1}$  can be detected by applying the SISO equalizer on  $\hat{\mathbf{y}}_k^{(B)}$  and  $\mathbf{C}_0 \cdot \mathbf{F}$ , with the extrinsic information  $\eta_{n(k-1)}(i)$  from the forward SSIC as the *a priori* information at the equalizer input. In the backward SSIC process,  $\mathbf{C}_1$  is used for IBI cancellation and  $\mathbf{C}_0$  is used for CCI cancellation. Replacing  $\mathbf{C}_1$  with  $\mathbf{C}_0$  during the SISO equalization will generate new information that is independent of what is obtained during the forward SSIC.

The combination of the forward SSIC and backward SSIC forms one iteration of the detection process. To summarize, during the forward SSIC detection,  $\mathbf{s}_{k-1}$  is detected before  $\mathbf{s}_k$ . The IBI is canceled by subtracting the *a posteriori* mean,  $\hat{\mathbf{s}}_{k-1}$ , from  $\mathbf{y}_k$  as in (5). Then the SISO equalizer is applied on  $\hat{\mathbf{y}}_k$  with the help of  $\mathbf{C}_1$  to get the *a posteriori* information for the IBI cancellation in the next block, and the extrinsic information to be used as the *a priori* input during the backward SSIC process. During the backward SSIC detection, the IBI is canceled by subtracting  $\hat{\mathbf{s}}_k$  as in (7), and the SISO equalizer is applied to  $\hat{\mathbf{y}}_k^{(B)}$  with the help of  $\mathbf{C}_0$  to get the soft information of  $\mathbf{s}_{k-1}$ . The extrinsic information at the output of the SISO equalizer will be used as *a priori* input for the forward SSIC in the next iteration. During the forward SSIC of the first iteration, the *a priori* probability is assumed to be  $P(s_{nk}) = \frac{1}{S}$ . It will be shown by simulations that the iterative detection method almost achieves the performance of optimum trellis-based detections, but is with a much lower complexity.

It should be noted that in order to construct  $\mathbf{C}_0$  and  $\mathbf{C}_1$ , the receiver needs to know the relative delays among the asynchronous nodes. The receiver can estimate the relative node delays by the method described in [12].

#### IV. MAC LAYER ANALYSIS

In the MAC layer, the data stream of one user is divided into frames. The data frames are transmitted in succession, *i.e.*, no space is inserted between two consecutive frames unless there is no data to transmit. This is different from most traditional MAC schemes, where random intervals are inserted between the transmission of two frames to reduce the collision among the users. The R-OOAT scheme, on the other hand, adds silence periods inside a frame to reduce the collision. Using on-off transmission on the symbol level, instead of the duty-cycled transmission on the frame level, renders a special structure in the received signal. This special signal structure in the MAC layer enables the joint signal detection in the PHY layer as described in Section III, and it is instrumental to the collision-tolerance of the proposed MAC scheme.

After detection, the cyclic redundancy check (CRC) or parity check can be applied to the frame to detect if there is error in the detection. Frames with uncorrectable errors will be discarded and retransmitted. The R-OOAT can recover some of the collided frames with PHY layer detection, and only

retransmit those frames with uncorrectable errors. Such an operation determines that, under the same traffic load and signal-to-noise ratio (SNR), the probability of retransmission in R-OOAT is lower compared to conventional MAC schemes, where retransmission will occur whenever there is a collision or frame error at the receiver.

With the R-OOAT scheme, the average transmission load of one user, *i.e.*, the number of information bits transmitted per unit time per unit bandwidth is  $\frac{1}{M} \log_2(S)$  bps/Hz/user.

Due to the retransmission of frames with uncorrectable errors, the effective spectral efficiency of the system can be expressed as

$$\eta_{R-OOAT} = \frac{N}{M} (1 - FER_{R-OOAT}) \log_2(S), \quad (8)$$

where  $FER_{R-OOAT}$  is the frame error rate (FER) of the R-OOAT.

We compare the performance of the R-OOAT scheme to the well known slotted ALOHA MAC protocol with the same transmission load. In the slotted ALOHA MAC, the transmission interval between two consecutive frames from one node is assumed to follow an exponential distribution with mean  $\frac{T_f}{\lambda}$ , with  $T_f$  being the duration of one frame. At a given time slot, the probability that a node will transmit a frame is thus  $P_t = 1 - e^{-\lambda}$ . To compare the R-OOAT scheme with the slotted ALOHA, we set  $P_t = 1 - e^{-\lambda} = \frac{1}{M}$ , such that the two systems have the same average transmission load. A frame is successfully transmitted if the following two conditions are met simultaneously: 1) there is one and only one frame transmitted; and 2) the frame at the receiver can be successfully detected. Therefore, the spectral efficiency of the slotted ALOHA system with  $N$  users is

$$\eta_{ALOHA} = \frac{N}{M} \left(1 - \frac{1}{M}\right)^{N-1} (1 - FER_{ALOHA}) \log_2(S), \quad (9)$$

where  $FER_{ALOHA}$  is the *non-collision* FER of the uncollided frames in the slotted ALOHA system. It should be noted that under the same system configuration,  $FER_{ALOHA} \leq FER_{R-OOAT}$  because the R-OOAT system performs detection over the colliding signals at the receiver. At the mean time, with the iterative detection algorithm described in Section III, the difference between  $FER_{ALOHA}$  and  $FER_{R-OOAT}$  is usually very small. Our simulation results indicate that  $FER_{ALOHA}$  and  $FER_{R-OOAT}$  are on the same order of magnitude.

Comparing (8) to (9), we can see that  $\eta_{R-OOAT} \geq \eta_{ALOHA}$  if the following condition is met

$$\left(1 - \frac{1}{M}\right)^{N-1} \leq \frac{1 - FER_{R-OOAT}}{1 - FER_{ALOHA}}. \quad (10)$$

The above inequality is met for almost all the practical system configurations. Based on (10), Table 1 lists the maximum values of  $FER_{R-OOAT}$  for various values of  $FER_{ALOHA}$  and  $M$ , for a system with  $N = 10$  nodes. It can be seen from Table 1 that even when  $FER_{ALOHA} = 10^{-3}$  and  $M = 50$ , we will always have  $\eta_{R-OOAT} > \eta_{ALOHA}$  as long as  $FER_{R-OOAT} < 0.3331$ , which is 333 times higher than  $FER_{ALOHA}$ . Our simulation results indicate that  $FER_{ALOHA}$  and  $FER_{R-OOAT}$  are usually on the

Table 1 The maximum value of  $FER_{R-OOAT}$  such that  $\eta_{R-OOAT} > \eta_{ALOHA}$  ( $N = 10$ )

$M$	10	20	30	40	50
$FER_{ALOHA} = 10^{-3}$	0.8785	0.6419	0.4929	0.3979	0.3331
$FER_{ALOHA} = 10^{-2}$	0.8796	0.6451	0.4975	0.4033	0.3391
$FER_{ALOHA} = 10^{-1}$	0.8906	0.6774	0.5431	0.4576	0.3992

same order of magnitude, such that  $\frac{1 - FER_{R-OOAT}}{1 - FER_{ALOHA}} \approx 1$ . Thus  $\eta_{R-OOAT} > \eta_{ALOHA}$  can be achieved for almost all the practical system configurations. The above analysis is corroborated by simulation results presented in the next section.

## V. SIMULATION RESULTS

We first investigate the BER performance of a CT-MAC system with BPSK modulation,  $R = 4$  repetitions and  $M = 12$  sub-symbol positions per symbol period, for various number of users  $N$ . The results are shown in Fig. 2. When  $N = 1$ , there is no collision among users, and the results serve as a lower bound for the best possible performance of the system. The iterative detection method was performed with 3 iterations. For comparison, the result from the system with the optimum MLSE detection and  $N = 4$  is also shown in the figure. The simulation of the optimum detection of systems with  $N > 4$  is extremely time consuming, thus only the result with  $N = 4$  is shown in the figure. It is clear from the figure that the sub-optimum iterative detection can achieve a performance that is almost identical to its optimum counterpart. In addition, the sub-optimum iterative detection method can achieve a performance that is reasonably close to the lower bound for a large range of  $N$ . As a result, the system is highly tolerant to collisions at the receiver.

Fig. 3 demonstrates the impact of the number of iterations on the FER performance. There are 100 symbols per frame. The biggest improvement in the FER performance is achieved from the 1st iteration to the 2nd iteration. The performance improvement gradually diminishes as the number of iterations increases. The performance difference between the 3rd and 4th iterations is almost negligible. In addition, the benefit of iterations is more apparent at high  $E_b/N_0$ . When  $E_b/N_0 \leq 10$  dB, it is sufficient to use 2 iterations.

Fig. 4 compares the effective spectral efficiency between the R-OOAT system and the slotted ALOHA system, under various values of  $N$  and  $M$ . There are 100 symbols per frame. The R-OOAT system employs  $R = 4$  repetitions per symbol. The  $E_b/N_0$  for both systems are 10 dB. Both systems have the same transmission load defined by  $\frac{1}{M}$  bps/Hz/user. The optimum spectral efficiency of the R-OOAT system is significantly higher than that of the slotted ALOHA system. For the R-OOAT system, it is observed that the optimum spectral efficiency can be achieved when  $\frac{N}{M} \approx \frac{3}{2}$ , *e.g.*, when  $N = 24$ ,  $M = 16$ , the maximum spectral efficiency,  $\max(\eta_{R-OOAT}) = 0.7$  bps/Hz, is achieved. For the slotted ALOHA system, the optimum spectral efficiency is achieved when  $\frac{N}{M} \approx 1$ , with a maximum spectral efficiency of  $\max(\eta_{ALOHA}) = 0.3$  bps/Hz. Therefore, under the same transmission load, the R-OOAT system can support more

users and achieve a spectral efficiency more than twice of that of the slotted ALOHA.

### VI. CONCLUSION

A new PHY/MAC design has been proposed based on the framework of the CT-MAC with R-OOAT. In the PHY layer, a sub-optimum iterative detection method has been proposed to extract the information from signals colliding at the receiver. The iterative detection has been developed by utilizing the special signal structure of the R-OOAT. It can achieve a performance very close to the trellis-based optimum detection, but is with a much lower complexity. In the MAC layer, the spectral efficiency has been analyzed and compared to the well-known slotted ALOHA scheme. Both analytical and simulation results have demonstrated that the new PHY/MAC operations can support more users and achieve a much higher spectral efficiency compared to the slotted ALOHA scheme.

### REFERENCES

- [1] A. El Fawal, J.-Y. Le Boudec, R. Merz, B. Radunovic, J. Widmer, and G. M. Maggio, "Trade-off analysis of PHY-aware MAC in low-rate low-power UWB networks," *IEEE Trans. Wireless Commun.*, vol. 7, pp. 4596 - 4607, Nov. 2008.
- [2] U. C. Kozat, U.C., I. Koutsopoulos, and L. Tassiulas, "A framework for cross-layer design of energy-efficient communication with QoS provisioning in multi-hop wireless networks," in *Proc. IEEE INFOCOM 2004*, vol. 2, pp. 1446 - 1456, 2004.
- [3] X. Lin, N. B. Shroff, and R. Srikant, "A tutorial on cross-layer optimization in wireless networks," *IEEE J. Selected Areas Commun.*, vol. 24, pp. 1452 - 1463, Aug. 2006.
- [4] G. Mergen and L. Tong, "Receiver controlled medium access in multihop ad hoc networks with multipacket reception," in *Proc. IEEE Military Commun. Conf. MILCOM 2001*, vol. 2, pp. 1014 - 1018, 2001.
- [5] L. Tong, V. Naware, and P. Venkatasubramanian, "Signal processing in random access," *IEEE Sig. processing Mag.*, vol. 21, pp. 29 - 39, Sept. 2004.
- [6] R. Samano-Robles, M. Ghogho, and D. C. McLernon, "An infinite user model for random access protocols assisted by multipacket reception and retransmission diversity," in *Proc. IEEE Sig. Processing Advances Wireless Commun. SPAWC 2008*, pp. 111 - 115, 2008.
- [7] B. Lu, X. Wang, and J. Zhang, "Throughput of CDMA data networks with multiuser detection, ARQ, and packet combining," *IEEE Trans. Wireless Commun.*, vol. 3, pp. 1576 - 1589, Sept. 2004.
- [8] R. Merz, J. Widmer, J.-Y. Le Boudec, and B. Radunovic, "A joint PHY/MAC architecture for low-radiated power TH-UWB wireless ad hoc networks," *Wireless Commun. Mobile Computing*, vol. 5, pp. 567 - 580, 2005.
- [9] P. Casari, M. Levorato, and M. Zorzi, "On the implications of layered space-time multiuser detection on the design of MAC protocols for ad hoc networks," in *Proc. Intern. Symp. Personal, Indoor Mobile Radio Commun. PIMRC'05*, vol. 2, pp. 1354 - 1360, 2005.
- [10] P. Casari, M. Levorato, and M. Zorzi, "MAC/PHY cross-layer design of MIMO ad hoc networks with layered multiuser detection," *IEEE Trans. Wireless Commun.*, vol. 7, pp. 4596 - 4607, Nov. 2008.
- [11] J. Wu and Y. Li, "Low power collision-tolerant media access control with on-off accumulative transmission," in *Proc. IEEE Intern. Conf. Commun. ICC'10*, May 2010.
- [12] J. Wu and Y. Li, "Random on-off accumulative transmission for asynchronous wireless sensor networks," in *Proc. IEEE Global Telecommun. Conf. Globecom'10*, Dec. 2010.
- [13] J. Wu and Y. R. Zheng, "Low complexity soft-input soft-output block decision feedback equalization," *IEEE J. Selected Areas Commun.*, vol. 26, pp. 281-289, 2008.

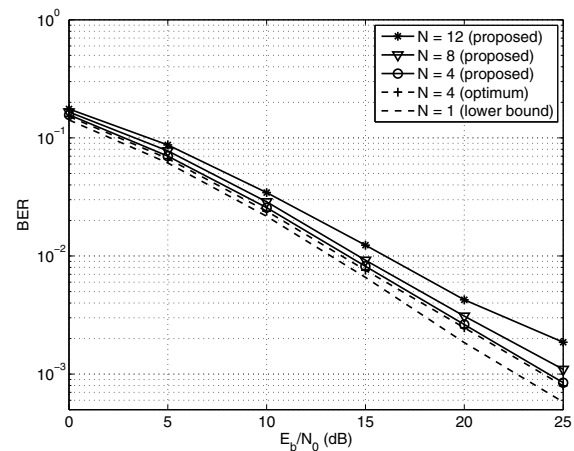


Fig. 2. BER performance of a system with  $M = 12$  sub-symbol positions per symbol,  $R = 4$  repetitions, and various number of nodes.

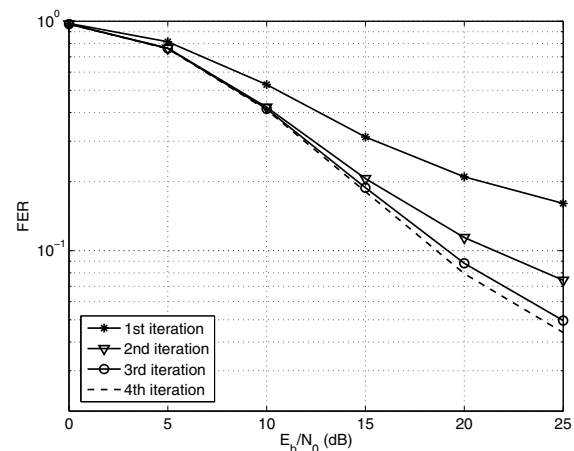


Fig. 3. FER performance of a system with  $N = 12$  users,  $M = 12$  sub-symbol positions per symbol, and  $R = 4$  repetitions.

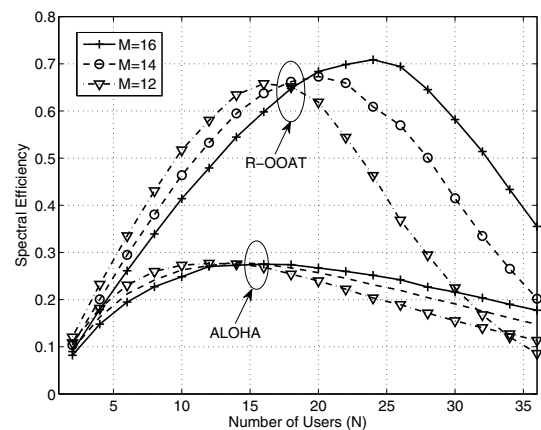


Fig. 4. Spectral efficiency v.s. number of users